Received 10 October 2019; revised 9 January 2020; accepted 23 January 2020. Date of publication 29 January 2020;
date of current version 27 April 2020. The review of this article was arranged by Editor A. Escobosa.

Digital Object Identifier 10.1109/JEDS.2020.2970177

Parameter Extraction and Compact Modeling of 1/f Noise for Amorphous ESL IGZO TFTs

WONDWOSEN E. MUHEA [1], GERARD U. CASTILLO [1], HAROLD C. ORDOÑEZ [1], THOMAS GNEITING [2] (Member, IEEE), GERARD GHIBAUDO [3] (Fellow, IEEE), AND BENJAMIN IÑIGUEZ [1] (Fellow, IEEE)

1 Department of Electrical, Electronics Engineering and Automachine, Universitat Rovira i Virgili, 43007 Tarragona, Spain
2 AdMOS GmbH, Advanced Modeling Solutions, 72636 Frickenhausen, Germany
3 IMEP-LAHC, INPG - Minatec, 38016 Grenoble, France

CORRESPONDING AUTHOR: W. E. MUHEA (e-mail: wmuhea@gmail.com)

This work was supported in part by the FI-Agaur Catalan Government Scholarship Program under Grant F I _B2_00129, and in part by 645760—DOMINO—H2020-MSCA-RISE-2014 (“DOMINO Project”), a MSCA-RISE-2014 European Project, and Project RTI2018-096019-B-C31 by the Spanish Ministry of Science.

ABSTRACT In this paper, the flicker noise properties of bottom-gate ESL structured amorphous InGaZnO (a-IGZO) thin-film transistors (TFTs) from two different technologies have been studied and modeled. Model development is carried out by adapting the Unified Model parameter Extraction Method (UMEM), developed for parameter extraction and compact modeling of TFT devices, and the unified 1/f noise model. Furthermore, comparative study of device figures of merits is performed to point out the device performance enhancements that the different fabrication technologies have brought about. It is found out that both devices have low deep state density, whereas the second device demonstrated higher performance in terms of carrier mobility and subthreshold slope. Both the DC and noise models are validated by matching them against experimental data obtained in different regimes of device operation.

INDEX TERMS a-IGZO, flicker noise, model, TFT.

I. INTRODUCTION

Amorphous InGaZnO thin-film transistors (a-IGZO TFTs) have drawn tremendous attention due to their higher carrier mobility, better bias stability, and large area uniformity of electrical properties. Such remarkable performance traits find a-IGZO TFTs a place in the design of flexible and transparent electronic circuits for a wide range of applications targeting technologies in consumer electronics, business, transportation, and military areas [1]. In particular, they outperform hydrogenated amorphous Silicon (a-Si:H) and become better substitutes to design driving and switching circuits for flat-panel flexible displays, and large area integrated circuit technologies [2]–[4].

As a-IGZO TFTs continue to appear in varieties of structures, electrical characterization of the devices is currently an active area of research to help better understanding of the device physics. Study of low-frequency noise behavior is an ideal tool in that regard for reasons such as to identify charge transport mechanism within the active layer, evaluation of interfacial trap states, etc. Furthermore, physics-based modeling of these devices plays vital roles in the design of highly efficient TFT based circuits for the mentioned applications.

Flicker noise characterization of a-IGZO TFTs with different sizes of the active layer have been reported during the last years [5]–[7]. The majority of the studies concern devices with a-IGZO thin film as thick as 50 μm or more. In contrast to that, compact modeling of 1/f noise in a-IGZO TFT devices with ESL layer and a very thin IGZO film was recently published by our group [8]. We targeted, in the work, investigation of the flicker noise mechanism as well as the effect of temperature on I-V, and noise properties of the scrutinized devices. We showed that the physical origin of noise in the devices is carrier number fluctuation due to the exchange of carriers between the dielectric-oxide traps and the channel. A slight correlated mobility variation was also observed at higher drain current region due to the modulation of carrier scattering by the variation of oxide interfacial charge. Based on this finding, a Unified Model parameter Extraction Method (UMEM) based 1/f noise model for

This work is licensed under a Creative Commons Attribution 4.0 License. For more information, see https://creativecommons.org/licenses/by/4.0/

a-IGZO TFT device was proposed by adapting the unified 1/f noise theory [8].

Using a similar approach, here, we have modeled the DC, and 1/f noise behavior of ESL-IGZO devices fabricated using different technologies. Performance-wise comparative study of the devices is presented as well. Section II of the paper briefly describes the UMEM based TFT I-V characteristics modeling followed by a succinct introduction of the well-known MOSFET flicker noise theories in Section III. Discussion of modeling, as well as device performance comparison results, are presented in Section IV, and a conclusion is drawn in Section V.

II. MODEL DESCRIPTION

UMEM based modeling of the I-V characteristics of a-IGZO TFT devices is based on assuming a two exponential density of states (DOS), i.e., the tail and deep state density. This splits the device operating regime into Above threshold (Fermi level is in the tail states), the subthreshold (Fermi level is in the deep states), and deep subthreshold (wherein diffusion transport is dominant). Separate I-V models developed for each regime are then bound together to form a simple I-V expression valid for all.

According to this approach, the above threshold current is given by [9]

$$I_{ab} = \frac{\frac{K}{V_{aa}^{\gamma_a}}(V_{GS} - V_T)^{1+\gamma_a} V_{DSe}\big(1 + \lambda(|V_{DS}| - V_{Dsat})\big)}{1 + R.\frac{K}{V_{aa}^{\gamma_a}}(V_{GS} - V_T)^{1+\gamma_a}} \quad (1)$$

where $K = \frac{W}{L}\mu_0 C_i$, W and L are the gate width and channel length respectively, V_T is the threshold voltage, C_i is the gate oxide capacitance density, V_{aa} and γ_a are extracted parameters that define the variation of the effective mobility with the applied gate voltage V_{GS}. V_{DS} is the drain voltage, R is the series resistance, and λ is the channel length modulation parameter.

The V_{Dsat} and V_{DSe} terms in (1) represent the saturation voltage and the transition from the linear to the saturation region and are defined respectively by [9]

$$V_{Dsat} = \alpha_s(V_{GS} - V_T) \quad (2)$$

$$V_{DSe} = V_{DS}\left[1 + \left(\frac{V_{DS}}{\alpha(V_{GS} - V_T)}\right)^m\right]^{\frac{-1}{m}} \quad (3)$$

where α_s and m are the saturation parameter and a parameter that determines the knee region in output characteristics respectively.

The parameters V_T, V_{aa}, and γ_a are extracted from the linear I-V transfer characteristics experimental data while α_s, and λ and m are obtained from the saturation transfer and output I-V measurement data respectively as per the procedures discussed in [9].

In the subthreshold regime (Fermi level is in the deep states) of operation of a-IGZO TFT devices ($V_{GS} < V_T$), the mobile charge carriers are less in number, and the drain current takes the form [9]

$$I_{bt}(V_{GS}, V_{DS1}) = K\left[\frac{(V_{GS} - V_{FB})^{\gamma_b}}{V_{bb}^{\gamma_b}}\right]V_{DSe1} \quad (4)$$

where V_{FB} is the flatband voltage, γ_b and V_{bb} are empirical model parameters that define the mobility variation in the subthreshold regime and are extracted from the linear transfer I-V data in the same way as the above threshold model parameters. V_{DSe1} is the transition function defined using (3) by replacing V_T with V_{FB}.

For a transistor operating in the deep subthreshold (well below V_T) regime, carrier diffusion transport mechanism dominates and the drain current is an exponential function of the gate voltage with the form [9]

$$I_S = I_{bt}(V_1, V_{DS1})e^{2.3\left(\frac{V_{GS}-(V_{FB}+V_1)}{S}\right)} \quad (5)$$

where S is the subthreshold slope, $V_{FB} + V_1$ is a voltage value slightly above the flat-band voltage for better sewing of I_{bt} and I_S.

In order to develop a single continuous drain current model, the expressions in (1), (6), and (8), are sewed together using a weighted tanh function in the order of increasing drain current magnitude. First, the total subthreshold regime drain current is evaluated from sewing the expressions in (4) and (5) as [9]

$$I_{sub} = \frac{|I_S|}{2}\left(1 - \tanh\left[\big(V_{GS} - (V_{FB} + V_1)Q_1\right]\right) + \frac{|I_{bt}|}{2}\left(1 + \tanh\left[\big(V_{GS} - (V_{FB} + V_1)\big)Q_1\right]\right) \quad (6)$$

where Q_1 is the weight of the tanh function, $(V_{FB}+V_1)$ is the point slightly above the flatband voltage selected for continuous transition of the drain current from deep-subthreshold to subthreshold regimes. Similarly, the total subthreshold current I_{sub} is sewed with the above threshold current I_{ab}, and the off-current is added to give the total drain current I_{DS} which reads [9]

$$I_{DS} = |I_o| + \frac{|I_{sub}|}{2}\left(1 - \tanh\left[\big(V_{GS} - (V_T + V_0)Q_2\right]\right) + \frac{|I_{ab}|}{2}\left(1 + \tanh\left[\big(V_{GS} - (V_T + V_0)\big)Q_2\right]\right) \quad (7)$$

where V_T+V_0 is a point above the threshold voltage adjusted to give sufficient continuity of the total drain current during the transition from subthreshold to above threshold regime of operation.

III. MOSFET FLICKER NOISE THEORIES

The several decades-long studies of the physical origin of flicker noise in semiconductors devices led to the two major theories that explain how 1/f noise is generated in FETs. These are the carrier number fluctuation theory (ΔN),

which related to the McWhorter charge trapping and de-trapping model [10], and the mobility fluctuation($\Delta\mu$) theory developed based on Hooge's hypothesis [11].

The former states that 1/f noise stems from the random change in carrier number within the channel of transistors due to the random capture/release of charge by the gate-oxide slow traps from/to the channel. Such process results in the fluctuation of channel/oxide interface charge (δQ_{it}) which is transferred to the flatband voltage via $\delta V_{fb} = \delta Q_{it}/WLC_{ox}$. Furthermore, the interfacial charge fluctuation modulates the carrier scattering rate causing a correlated variation of the carrier mobility $\delta\mu_{eff}$. The resulting fluctuation in the drain current (δI_{ds}) due to these effects reads [12]–[14]

$$\delta I_{ds} = -g_m \delta V_{fb} - \alpha I_{ds} \mu_{eff} \delta Q_{it} \tag{8}$$

where g_m is the transconductance. Evaluation of the normalized current noise power spectral density (PSD) from (8) gives [13]–[15]

$$\frac{S_{Id}(f)}{I_{DS}^2} = \left[1 \pm \alpha_c \mu_{eff} C_i \frac{I_{DS}}{g_m}\right]^2 \left[\frac{g_m}{I_{DS}}\right]^2 S_{Vfb} \tag{9}$$

where the S_{Vfb} represents the bias independent flatband voltage noise spectral density which takes the form [14]–[17]

$$S_{Vfb} = \frac{q^2 kT \lambda_s N_{st}}{WLC_i^2 f} \tag{10}$$

where λ_s is the tunneling attenuation distance ($\simeq$ 0.1nm), and N_{st} is volume insulator trap density.

The mobility fluctuation theory, on the other hand, concerns that the 1/f noise generated in FET devices with the random change in carriers' effective mobility due to phonon number fluctuations. The normalized power spectral density of the drain current noise is defined as [11], [13]–[15], [18]

$$\frac{S_{Id}(f)}{I_{DS}^2} = \frac{q\alpha_h}{WLQ_i f} \tag{11}$$

where q is the elementary charge, α_h is the Hooge parameter, and Q_i is the channel charge. Eqn (11) holds true for devices operating in the linear regime, whereas an expression that is valid for non-linear device operation is presented in as [14], [18]

$$\frac{S_{Id}(f)}{I_{DS}^2} = \frac{q\alpha_h \langle\mu_{eff}\rangle V_d}{fL^2 I_{DS}} \tag{12}$$

where $\langle\mu_{eff}\rangle$ is the average carrier mobility. One can see that the expression in (11) is a reduced version of (12) in the linear regime of operation.

From the model definitions in (9) and (12), it is apparent that the origin of flicker noise in a given device can be identified through investigation of how the $\frac{S_{Id}(f)}{I_{DS}^2}$ varies with respect to the drain current. A $\frac{S_{Id}(f)}{I_{DS}^2}$ that is found to be proportional to the squared $\frac{g_m}{I_{DS}}$ over a wide range of I_{DS} reflects that carrier number fluctuation is the principal origin of flicker noise, whereas an inverse relationship between the normalized noise PSD and drain current confirms the mobility fluctuation as the prevailing noise mechanism in any device under study.

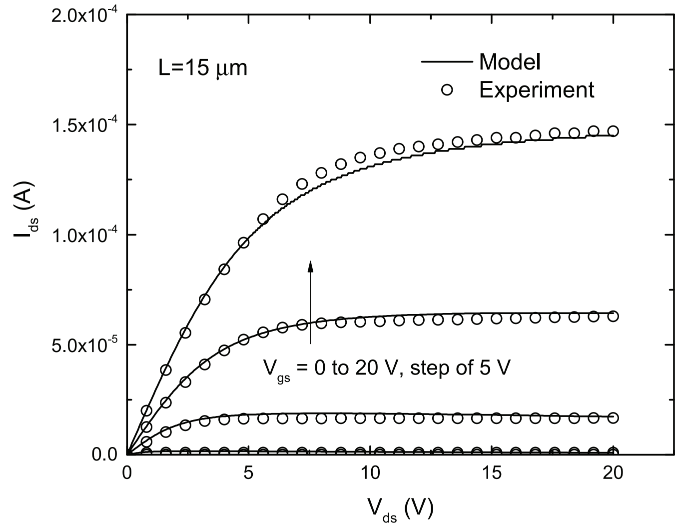

FIGURE 1. Model-experimental data comparison for the output I-V characteristics of 15 × 100μm^2 device (First generation device).

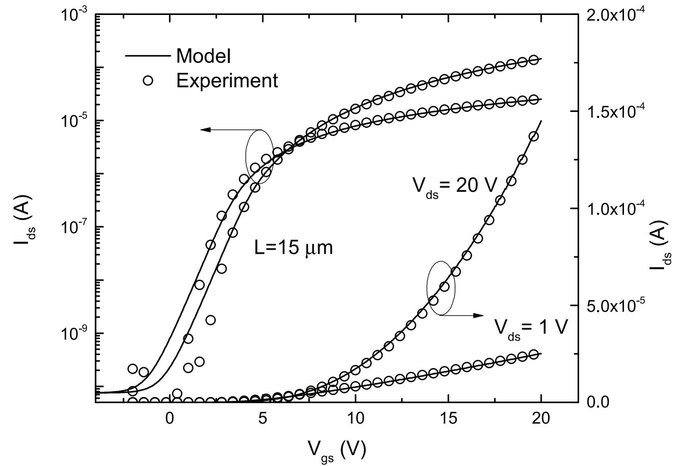

FIGURE 2. Model-experimental data comparison for the transfer I-V characteristics of 15 × 100μm^2 device (First generation device).

IV. RESULTS AND DISCUSSION

The I-V and low-frequency noise characteristics of two bottom-gate ESL a-IGZO devices fabricated using different technologies have been investigated and modeled. The devices have a 200 nm thick dielectric layer, a 100 nm thick ESL, and a 12 nm thick IGZO layer.

It is apparent from the I-V characteristics in Fig. 1 and Fig. 2 that the first generation device exhibits a positive shift in the threshold voltage (V_{th}) when entering to saturation regime. That is presumably due to a high density of traps existing in the amorphous channel material. On the other hand, the device from the second technology, i.e., the 20 μm device (see Fig. 3 and Fig. 4), demonstrated better performance over the first, the 15 μm (see Fig. 1 and Fig. 2)

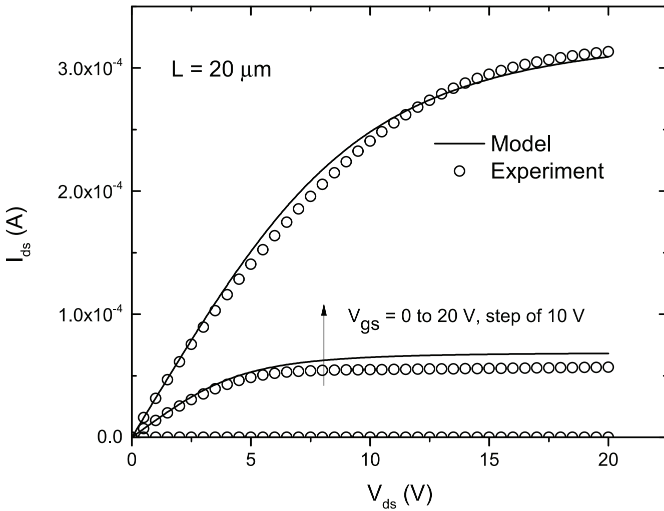

FIGURE 3. Model-experimental data comparison for the output I-V characteristics of 20 × 100μm^2 device (Latest generation device).

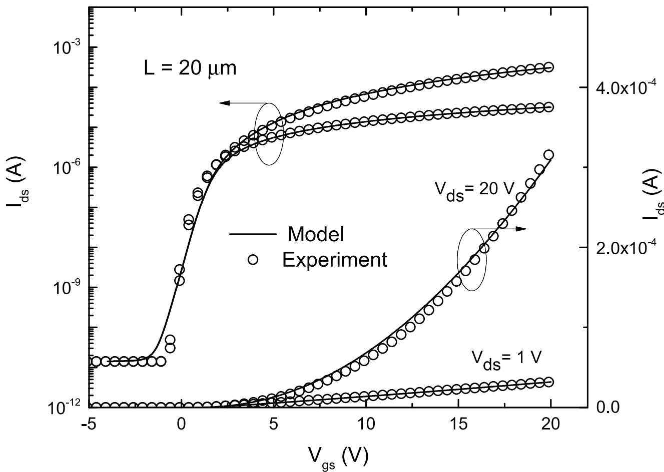

FIGURE 4. Model-experimental data comparison for the transfer I-V characteristics of 20 × 100μm^2 device (Latest generation device).

TABLE 1. Empirical and extracted model parameter values.

Parameter	Description	Values	
W (μm)	Device Width	100	
L (μm)	Device Length	15	20
V_{th} (V)	Threshold voltage	3.04	0.82
V_{FB} (V)	Flatband voltage	2.23	0.33
μ_{eff} $(cm^2V^{-1}s^{-1})$	Mobility at maximum gate voltage	10.8	15.9
α_s	Saturation parameter	0.35	0.54
γa	Mobility parameter	0.26	0.126
m	Transition parameter	2.14	2.4
λ	Channel length modulation	0.0085	0.0028
δ	Frequency exponent	1.05	1.1
$\alpha \times 10^5$ (VsC^{-1})	Scattering coefficient	2.2	0.0
$N_{st} \times 10^{11}$ $(eV^{-1}cm^{-2})$	Oxide trap density	4.15	3.85
S (Dec/V)	Subthreshold Slope	2.2	2.7
$N_{ga} \times 10^{17}$ $(cm^{-3}eV^{-1})$	Deep state density	1.1	1.9

with increased effective mobility, a higher drain current, and improved subthreshold slope as reported in Table 1.

Both generations of the investigated ESL a-IGZO devices exhibit low deep state density. In such a case, the subthreshold current defined by (5) can be neglected in the I-V modeling if the flatband voltage (V_{FB}) is found to be close enough to the threshold voltage of the device. From the V_{FB} and V_{th} parameters listed in Table 1, one can see that the difference between the values is smaller in the 20 μm device than in the 15 μm device. As a result, the subthreshold current model given by (5) is omitted in the DC model of the 20 μm device. That keeps the I-V model simple. The excellent model-experimental data agreement achieved in the output and transfer characteristics of the devices, in all regimes of operation, validates the UMEM based modeling.

Study of the trend of the 1/f noise experimental data PSD against drain current reveals the normalized PSD follows the squared transconductance drain current ratio over a wide span of drain current (see the insets in Fig. 5 and Fig. 6). Thus, carrier number fluctuation is found to be the principal flicker noise mechanism in both generations of devices. An additional noise coming from correlated mobility fluctuation is observed in the device from the previous technology (the 15μm) at higher drain current regions.

Based on the analysis result, the unified flicker noise model is developed. The relation between normalized current noise PSD and drain current is illustrated in Fig. 5 and Fig. 6 along with the corresponding transconductance-current ratio squared for the 15 μm and 20 μm devices respectively. A similar trend is observed between the two functions over three to four decades of I_{DS}. The model correlates well with the experimental data in both cases. Such a result supports the conclusion that the measured 1/f noise originates mainly from the carrier number fluctuation within the channel. It is also confirmed that the model sufficiently reproduces the experimental data wherever the additional effect of correlated mobility fluctuation is present or not. That shows the model captures the device physics.

Furthermore, noise simulations in the frequency domain are carried out for both devices in the subthreshold, linear, and saturation operation regimes, and the results are presented in Fig. 7 and Fig. 8. A clear $1/f^{\delta}$ frequency behavior is observed in the noise spectrum in the considered regions of operation with a power factor of δ close to unity, in general. However, in the case of the 20 μm device, there is a noticeable deviation of the noise PSD from the expected behavior in the low-frequency region. That may be ascribed to the presence of fewer defects as we go deep inside the oxide. The good agreement achieved between the measured and modeled normalized current noise PSD over a range of frequencies and bias points validates the proposed model.

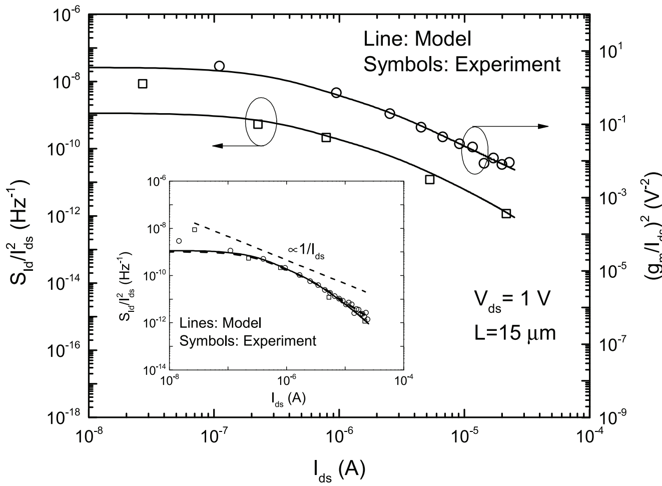

FIGURE 5. Plot of model-experimental data comparison for $\frac{Sid}{I_{ds}^2}$ (left) and $[\frac{gm}{I_{ds}}]^2$ (right) with respect to drain current for the 15 × 100μm^2 device. $V_{ds} = 1$ V.

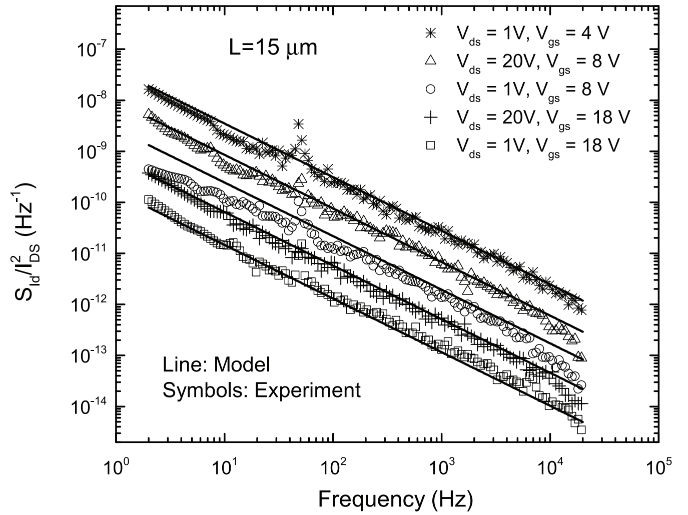

FIGURE 7. Measured and modeled normalized 1/f noise power spectral density of 15 × 100μm^2 device over a range of frequencies in subthreshold, linear, and saturation region.

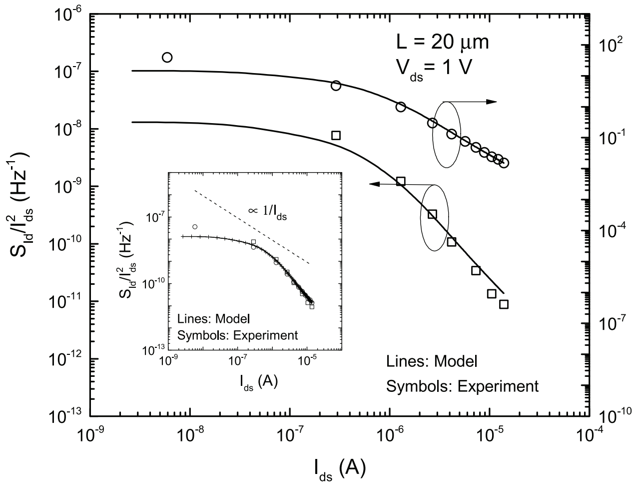

FIGURE 6. Plot of model-experimental data comparison for $\frac{Sid}{I_{ds}^2}$ (left) and $[\frac{gm}{I_{ds}}]^2$ (right) with respect to drain current for the 20 × 100μm^2 device. $V_{ds} = 1$ V.

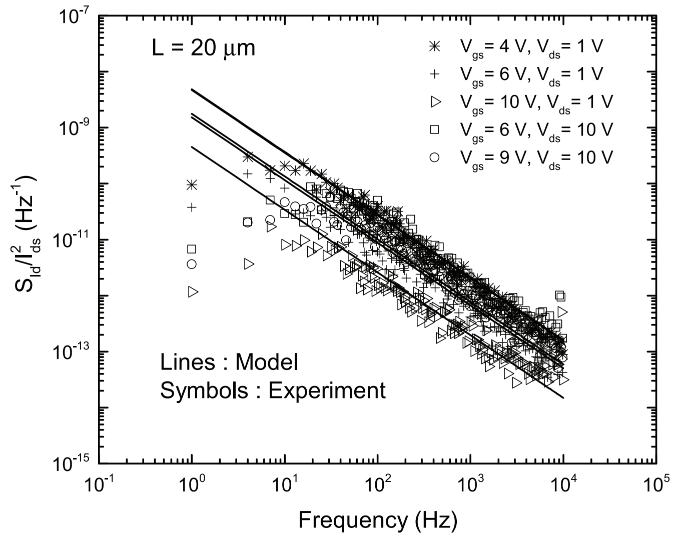

FIGURE 8. Measured and modeled normalized 1/f noise power spectral density of 20 × 100μm^2 device over a range of frequencies in subthreshold, linear, and saturation region.

In the end, we found it relevant to remark that in contrast to previously reported works on 1/f noise analysis in a-IGZO TFTs [5]–[7] (which use modeling or parameter extraction methods developed for crystalline MOS devices), our study is fully based on modeling and parameter extraction methods developed specifically for IGZO TFTs. Moreover, performance-wise comparison of the devices from the two technologies unveiled that the second group of devices has improved I-V and noise performance and stability (concerning the unwanted threshold voltage variation).

V. CONCLUSION

A physics-based low-frequency noise model for bottom gate ESL a-IGZO TFT devices is presented in this paper. The normalized 1/f noise PSD with respect to drain current and frequency is investigated in a log-log scale. The results show that the PSD varies similarly to the squared transconductance to drain current ratio over a wide-spanning of the drain current. Thus, the random change in carrier number within the channel appeared to be the source of the measured 1/f noise. The excellent model and experimental data agreement in the I-V and 1/f noise characteristics proved the accuracy and solid physics foundation of the proposed model.

ACKNOWLEDGMENT

The authors would like to thank TNO laboratory for providing the fabricated devices and AdMOS company and IMEP-LAHC for arranging the measurement systems.

REFERENCES

[1] J.-S. Park, J. K. Jeong, Y.-G. Mo, and H. D. Kim, "Improvements in the device characteristics of amorphous indium gallium zinc oxide thin-film transistors by Ar plasma treatment," *Appl. Phys. Lett.*, vol. 90, no. 26, Jun. 2007, Art. no. 262106.

[2] O. Moldovan, A. Castro-Carranza, M. Estrada, A. Cerdeira, F. Lime, and B. Iñiguez, "A complete charge-based capacitance model for IGZO TFTs," *IEEE Electron Device Lett.*, vol. 40, no. 5, pp. 730–733, May 2019.

[3] J. S. Park, W.-J. Maeng, H.-S. Kim, and J.-S. Park, "Review of recent developments in amorphous oxide semiconductor thin-film transistor devices," *Thin Solid Films*, vol. 520, no. 6, pp. 1679–1693, Jan. 2012.

[4] T. Kamiya, K. Nomura, and H. Hosono, "Present status of amorphous In-Ga-Zn-O thin-film transistors," vol. 11, no. 4, Feb. 2010, Art. no. 044305.

[5] T.-C. Fung, G. Baek, and J. Kanicki, "Low frequency noise in long channel amorphous In-Ga-Zn-O thin film transistors," *J. Appl. Phys.*, vol. 108, no. 7, Oct. 2010, Art. no. 074518.

[6] J. C. Park *et al.*, "Low-frequency noise in amorphous indium-gallium-zinc oxide thin-film transistors from subthreshold to saturation," *Appl. Phys. Lett.*, vol. 97, no. 12, Sep. 2010, Art. no. 122104.

[7] Y. Liu, H. He, R. Chen, Y.-F. En, B. Li, and Y.-Q. Chen, "Analysis and simulation of low-frequency noise in indium-zinc-oxide thin-film transistors," *IEEE J. Electron Devices Soc.*, vol. 6, no. 1, pp. 271–279, Jan. 2018.

[8] W. E. Muhea, T. Gneiting, and B. Iñiguez, "Current-voltage and flicker noise analysis and unified modeling for amorphous indium-gallium-zinc-oxide thin film transistors with etch stop layer from 298 to 333 K," *J. Appl. Phys.*, vol. 125, no. 14, Apr. 2019, Art. no. 144502.

[9] O. Moldovan *et al.*, "A compact model and direct parameters extraction techniques for amorphous gallium-indium-zinc-oxide thin film transistors," *Solid-State Electron.*, vol. 126, pp. 81–86, Dec. 2016.

[10] A. L. McWhorter, *1/F Noise and Germanium Surface Properties*. Philadelphia, PA, USA: Univ. Pensylv. Press, 1957, pp. 207–228.

[11] F. Hooge, "1/f noise is no surface effect," *Phys. Lett. A*, vol. 29, no. 3, pp. 139–140, Apr. 1969.

[12] G. Ghibaudo, "On the theory of carrier number fluctuations in MOS devices," *Solid-State Electron.*, vol. 32, no. 7, pp. 563–565, 1989.

[13] G. Ghibaudo, O. Roux, C. Nguyen-Duc, F. Balestra, and J. Brini, "Improved analysis of low frequency noise in field-effect MOS transistors," *Physica Status Solidi (a)*, vol. 124, no. 2, pp. 571–581, Apr. 1991.

[14] G. Ghibaudo and T. Boutchacha, "Electrical noise and RTS fluctuations in advanced CMOS devices," *Microelectron. Rel.*, vol. 42, no. 4–5, pp. 573–582, Apr. 2002.

[15] T. Boutchacha, G. Ghibaudo, and B. Belmekki, "Study of low frequency noise in the 0.18 μm silicon CMOS transistors," in *Proc. IEEE Int. Conf. Microelectron. Test Struc.*, 1999, pp. 84–88.

[16] G. Ghibaudo, O. Roux-dit-Buisson, and J. Brini, "Impact of scaling down on low frequency noise in silicon MOS transistors," *Physica Status Solidi (a)*, vol. 132, no. 2, pp. 501–507, Aug. 1992.

[17] S. Christensson, I. Lundström, and C. Svensson, "Low frequency noise in MOS transistors—I theory," *Solid-State Electron.*, vol. 11, no. 9, pp. 797–812, Sep. 1968.

[18] I. M. Hafez, G. Ghibaudo, and F. Balestra, "A study of flicker noise in MOS transistors operated at room and liquid helium temperatures," *Solid-State Electron.*, vol. 33, no. 12, pp. 1525–1529, Dec. 1990.